Research Square

Preprints are preliminary reports that have not undergone peer review.
They should not be considered conclusive, used to inform clinical practice,
or referenced by the media as validated information.

A Label-free, Fast and High-specificity Technique for Plant Cell Wall Imaging and Composition Analysis

Huimin Xu
China Agricultural University
Yuanyuan Zhao
Beijing Forestry University
Yuanzhen Suo
Peking University
Yayu Guo
Beijing Forestry University
Yi Man
Beijing Forestry University
Yanping Jing
Beijing Forestry University
Xinqiang He
Peking University
Jinxing Lin (linjx@ibcas.ac.cn)
Institute of Botany, Chinese Academy of Sciences, Beijing 100093, China. https://orcid.org/0000-0001-9338-1356

Methodology

Keywords: CRS, CARS, SRS, cell wall, label-free, chemical composition

Posted Date: November 19th, 2020

DOI: https://doi.org/10.21203/rs.3.rs-107437/v1

License: This work is licensed under a Creative Commons Attribution 4.0 International License.
Read Full License

Version of Record: A version of this preprint was published on March 19th, 2021. See the published version at https://doi.org/10.1186/s13007-021-00730-9.

Abstract

Background: Cell wall imaging can considerably permit direct visualization of the molecular architecture of cell walls and provide the detailed chemical information on wall polymers, which is imperative to better exploit and use the biomass polymers; however, detailed imaging and quantifying of the native composition and architecture in the cell wall remains challenging.

Results: Here, we describe a label-free imaging technology, coherent Raman scattering microscopy (CRS), including coherent anti-Stokes Raman scattering (CARS) microscopy and stimulated Raman scattering (SRS) microscopy, which images the major structures and chemical composition of plant cell walls. The major steps of the procedure are demonstrated, including sample preparation, setting the mapping parameters, analysis of spectral data, and image generation. Applying this rapid approach, which will help researchers understand the highly heterogeneous structures and organization of plant cell walls.

Conclusions: This method can potentially be incorporated into label-free microanalyses of plant cell wall chemical composition based on the *in situ* vibrations of molecules.

Background

Plant cell walls are renewable biomaterial composed of lignin and various polysaccharides. Due to the complex three-dimensional matrix, the chemical composition of plant cell walls can vary not only between tissues and cell types but also along developmental gradients and even within a single cell wall [1-3]. Therefore, major efforts are currently under way to explore cell wall composition and structure in the native state, mostly by applying high-resolution approaches at the scale of single cells or cell wall layers.

Over the past two decades, various plant cell wall imaging techniques have been developed to analyze plant cell wall microstructure and their chemical composition [4-8]. Such as bright- and dark-field microscopy [9], polarized light microscopy [10], transmission electron microscopy (TEM) [11], scanning electron microscopy (SEM) [11], and confocal microscopy [12]. Moreover, histochemical and immunolabeling techniques have been applied to investigate the dynamics of different plant wall polysaccharides [8,13,14]. Visualization of plant cell wall lignification using fluorescence-tagged monolignols has also been reported [15-17]. Furthermore, with the discovery of fluorescent proteins, the use of genetically encoded fusion proteins (combining a marker protein with a fluorescent protein) has become a useful method for labeling cell walls, enabling relatively simple visualization of the cell walls of living plants. In addition, some fluorescently labeled biological samples of plants for developmental and cellular were imaged by Light-sheet fluorescence, such as selective-plane illumination microscopy (SPIM) [18].This labeling technique served as a basis for the development of laser-scanning confocal microscopy and stimulated emission depletion microscopy imaging systems, which have significantly improved the temporal-spatial resolution and signal-to-noise ratio of cell wall imaging [19].

Rapid advances in imaging technology are improving our understanding of the spatial heterogeneity of individual cell walls, as well as taxonomic-level differences between cell walls [5]. For example, new, label-

free imaging techniques have evolved into powerful tools to detect and characterize the complex chemical and structural composition of the plant cell wall. Compositional information can be obtained through a variety of label-free imaging technologies, such as atomic force microscopy (AFM) [20-22], Fourier-transform infrared (FTIR) spectroscopy [6,23], and confocal Raman microscopy (CRM) [24-26]. However, cumbersome and time-consuming sample preparation, serious damage to samples, commonly non-quantitative and dynamic processes involved in the conversion cannot be followed at high spatiotemporal resolution [19].

Here, we present coherent Raman scattering (CRS) microscopy, including coherent anti-Stokes Raman scattering (CARS) microscopy and stimulated Raman scattering (SRS) microscopy, as an effective method for imaging complex chemistry of plant cell walls, based on molecular vibrations in biological molecules, which is free from sample autofluorescence interference, can observe substances that is hard to label and is not dependent on exogenous labels, such as lignin and large biomolecules. CARS microscopy offers a dramatic improvement in signal levels over spontaneous Raman microscopy, thus offering a significantly reduced scanning rate at several seconds per frame (512 × 512 pixels) and making video-rate imaging possible [27]. In addition, epi-detected CARS (E-CARS) microscopy with two synchronized picosecond pulse trains was reported to greatly improve the image contrast via an effective rejection of the solvent background [28,29]. SRS technology overcomes these limitations and fulfills the promise of useful vibrational contrast [30], offers a signal that is orders of magnitude stronger than spontaneous Raman microscopy, and exhibits straightforward image interpretation and quantification without complications from the non-resonant background and phase-matching conditions [31]. Because SRS is free of the non-resonant background, its signal intensity is linearly dependent on the analyte concentration only [12]. These merits make background-free, *in situ* quantitative microanalysis of cellular structure and chemical composition in live plant tissues possible [32,33]. Moreover, high-speed imaging makes it easy to capture a dynamic process in whole living cells and a diffraction-limited spatial resolution of ~350 nm and pixel dwell time of 50 μs [34].

Below we describe the necessary steps and typical obstacles encountered when attempting to quantify the chemical composition in plant cell walls. Then, we consider the process we used in our previously published work in more detail. This protocol will allow the interested reader to address fundamental questions regarding the chemical and structural composition of plant cell walls, genetically modified cell walls, and the biorefinery process.

Materials

Reagents

This protocol does not require specific reagents. Distilled water and ethyl alcohol are sufficient for sample preparation.

Equipment

- Sliding microtome (Leica SM2010 R)
- CRS microscope. The integrated CARS and SRS imaging system is a custom-built system with a commercial laser source (APE PicoEmerald, Germany) and an optimized inverted microscope (Olympus FV1000, Japan). The picosecond laser emits synchronized pump and Stokes beams. The pump beam is tunable from 700 to 990 nm and consists of an 80-MHz pulse train with 2-ps pulse width. The 1031-nm Stokes beam is modulated by a built-in electro-optic modulator (EOM) at 20 MHz. The pump and Stokes beams are overlapped and coupled into an inverted laser-scanning microscope optimized for near-infrared throughput. Non-descanned detectors are used for CARS imaging. A detector and a lock-in amplifier (customized from APE, Germany) are used for SRS imaging. This imaging system can perform CARS and SRS imaging simultaneously.

Software

- Fiji is an open-source image processing package based on ImageJ, which bundles together many plugins that facilitate scientific image analysis (https://imagej.net/Fiji).
- The FV10-ASW3.0 software is used to control the microscope (https://www.photonics.com/Product.aspx?PRID=47380).

Plant samples

Protocol

The present protocol consists of the following three main steps: sample preparation, acquisition of spectra, and computational analysis. Moreover, computational analysis can be semi-quantitative or fully quantitative.

Sample preparation

Tissues of herbaceous and woody plants can be used for CRS imaging. We recommend using at least three biological replicates, although more might be necessary depending on the question being addressed. If possible, use fresh samples or samples that have been kept at 4℃, or -80℃. Dried-out material is not suitable. The micro cuttings could be obtained with conventional microtechniques, allowing us to achieve better data quality by generating sections of equal thickness, which helps to produce sharp images and significantly reduces the risk of reporting inaccurate differences between samples. In our work, a sliding microtome (option a) was used to prepare woody and solid samples. Although no defined thickness is required for the analysis, it is crucial to have a planar surface with intact cell walls (as the inelastic scattering, not the absorption, is measured). Importantly, the interference from chloroplast fluorescence can be severe in some samples. Therefore, for many plant samples, appropriate embedding and chlorophyll removal is key, as described in detail below.

Acquisition of Spectra: CRS imaging settings

The laser intensity should be sufficiently high to obtain good counts per molecule (CPM), to ensure a good signal-to-noise ratio, but also sufficiently low to avoid photobleaching, photodamage, and saturation effects during the CRS measurement. The principle and design of CRS microscopy are shown in Figure1**.** In SRS, two laser beams at w_p and w_S coincide on the sample (Fig.1a). When the difference in frequency, $\Delta\omega = \omega_p - \omega_s$, also called the Raman shift, matches a particular molecular vibrational frequency w, amplification of the Raman signal is achieved by virtue of stimulated excitation. Consequently, the intensity of the Stokes beam, I_s, experiences a gain, ΔI_s (stimulated Raman). By contrast, unlike SRL and SRG, CARS exhibit a non-resonant background (Fig.1b). CARS microscopy achieves far stronger Raman signals, although suffers from a non-resonant electronic background that can limit the sensitivity for low concentration species. Fig.1c shows the experimental scheme used to image the plant cell wall, together with the chemical composition of stem and roots. Experimental scheme of the CRS images of plant cell wall composition were showed in Fig.1d.

Quantitative analysis of SRS-calibrated images

This section comprehensively describes the guidelines for image and data processing. The calibrated images allow an estimate of the protein distribution in specific cellular compartments, organelles, or structures. For that purpose, an additional fluorescent marker is used. Intensity analyses for specific types of the cell wall were performed with Fiji software. The program then selected pixels with intensity values above the set threshold for statistical analysis. For each type of plant sample, no less than three images were selected for intensity analysis. Lignin (1600 cm^{-1}) signals in each pixel were plotted. We recommend meticulously following the critical steps of the procedure, and researchers can optimize the analyses according to own needs.

Prepare the plant samples by Sliding microtome (Leica SM2010 R)

Timing: 30 min-1 h.

1. Clamp the specimen in the universal cassette clamp.
2. Replace the pressure plate; both the pressure plate and the matching insertion aid must be replaced.
3. To replace them, proceed as follows: push the knife guard toward the right and push the lever upward to release the clamp of the pressure plate.

**Note: Now carefully pull the insertion aid out and to the left. The pressure plate can now be taken off. To mount another pressure plate, please proceed in the reverse sequence. Only use the pressure plate together with the matching insertion aid.*

4. To loosen the clamp, rotate the eccentric lever upward,
   and orient the specimen in the cutting direction by turning the setscrews to orient the specimen.

**Note: Turning the lever further to the left re-clamps the orientation.*

5. When clamping a disposable blade, handle the microtome knives or blades carefully. The blade holder must be installed in the instrument before a blade is inserted.
6. Inserting the knife: Lock the knife sledge in place using the locking knob. Please make sure that the knife holder is firmly clamped using the clamping lever and that the knurled head screw is tightened. Push the knife guard to the right, and loosen the clamping screws sufficiently to allow the knife to be inserted. Take the knife out of the knife case and insert it carefully. Tighten the two clamping screws in alternation until both are secure, and cover the knife with the knife guard.
7. Cutting into the specimen (trimming). Adjust the section thickness setting, and then hold the knife sledge at the grip and place the sledge behind the specimen. The plant samples are cut into 10-μm-thick slices. These cross-sections are gently washed using distilled water.
8. Pull the knife guard of the blade/knife holder to the right. To feed the specimen towards the knife, turn the coarse drive wheel.
9. Select the required section thickness with the section thickness adjusting knob and move the manual feed lever. Each lever movement causes a specimen to feed by the selected amount.
10. Move the knife sledge back and forth until the specimen surface is trimmed, as required.

**Note: The blades are extremely sharp; careful attention is required.*

11. Collect the sections using a disposable plastic pipette during sectioning in the buffer tray. Alternatively, the sections can be transferred from the buffer tray into a glass beaker and then to a clear Petri plate. Then transferred the sections to the slide and seal the slide for CRS image (Fig.2).

Acquisition of CRSimages

Plant cell wall samples should be sectioned into slices and placed on glass slides. Spread the section on the slide with a fine brush and add one drop of fresh H_2O. Pick up a coverslip (cleaned with Kimwipes) with the help of a tweezer and carefully place it on top. Stick the corners of the coverslip to keep them from falling off when placed inversely on the microscope stage. Adjust the *X*–*Y* axes of the microscope stage to place the sample directly above the objective lens. Adjust the *Z* axis so that the sample is in the focal plane in the bright-field mode. CRS and imaging data can be collected.

**Note: Avoid air bubbles in the liquid film.The working distance of the objective lens is very short. Adjust the Z axis very carefully to avoid contact between the objective lens and the coverslip.*

Collecting CARS and imaging data, lignin (option e), cellulose (option f), and lipid (option g) of the cell wall as examples.

Timing: 0.1 h of setup, 0.2 h of measurement.

(e) Collecting CARS images of lignin

1. Set the wavelength of the pump beam at 885.5 nm by ticking “Set Signal”. The frequency difference of the pump and the Stokes beams is now at 1600 cm^{-1}, matching the aromatic ring vibration frequency of lignin.
2. Set the power of the pump and Stokes beams by ticking the “Set OPO Power” and the “Set IR Power” boxes, respectively. It is safe to set the power at 200 mW for each beam in this example.

**Note: When the laser power is too high, samples might be burned.*

3. Toggle the “OPO Signal”, the “Laser IR”, and the “System Shutter” buttons to let the pump and Stokes beams enter the microscope.
4. Move the stage and optimize the focus to identify an area containing the xylem cells of wood samples or herbaceous samples in the bright-field mode.
5. Set the scanning speed at 4.0 µs per pixel. Set the image size as 512 × 512 pixels. Check the RXD4 checkbox to activate the CARS channel. Deactivate other channels.
6. Begin scanning by clicking the “XY Repeat” (3). Finely adjust the *X*, *Y*, and *Z* axes to focus on the area of interest.

**Note: If there is no signal, increase the laser power and adjust the voltage of the NDD detector by changing the value of “HV” on the RXD4 channel. Make sure there are no overexposed pixels. The best laser power and “HV” value will generate the best contrast of CARS images.*

7. Check the “Kalman” checkbox in the “Filter Mode”. Type in “5” for the line average. Click the “XY” button to start CARS imaging. Save the image to your desired file path.
8. Background measurement. Toggle the “Laser IR” button in the laser control software to block the Stocks beam. Click the “XY” button to start CARS imaging. Save the image to a file path.
9. Repeat Steps 2-8 for imaging of different views.
10. Repeat Steps 2-9 for different samples.

(f) **Collecting CARS images of cellulose**

1. Set the wavelength of the pump beam at 926.5 nm by ticking the “Set Signal” box. The frequency difference of the pump and the Stokes beams is now at 1100 cm^{-1}, matching the C-O stretching vibration frequency of the polysaccharides.
2. Repeat Steps e (2-8) for imaging of different views.
3. Repeat Steps f (1-3) for different samples.

(g) Collecting CARS images of polysaccharides of suberin

1. Set the wavelength of the pump beam at 797.2 nm by ticking “Set Signal”. The frequency difference of the pump and the Stokes beams is now at 2850 cm^{-1}, matching the C-H stretching vibration frequency of the polysaccharides.

2. Repeat Steps e (2–8) for imaging of different views.
3. Repeat Steps g (1-3) for different samples.

Collecting SRS and imaging data for lignin (option h), cellulose (option i), and lipid (option j) of the cell wall, as examples.

Timing: 0.1 h of setup, 0.2 h of measurement.

(h) Collecting SRS images of lignin

1. Set the wavelength of the pump beam to 885.5 nm by ticking “Set Signal”. The frequency difference of the pump and the Stokes beams is now at 1600 cm^{-1}, matching the aromatic ring vibration frequency of lignin.
2. Activate the built-in electro-optic modulator by toggling the “EOM” button in the “EOM Control” software.
3. Set the power of the pump and Stokes beams by ticking the “Set OPO Power” and “Set IR Power” boxes, respectively. It is safe to set the power at 200 mW for each beam in this example.

Note: When the laser power is too high, samples might be burned.

4. Toggle the “OPO Signal”, “Laser IR”, and “System Shutter” buttons to let the pump and Stokes beams enter the microscope.
5. Open the control software of the SRS detection module (Fig.3). Set the integral time as 2 μs. The “SEED” indicator should be green if the lock-in amplifier of the detection module is connected correctly.

**Note: The “SEED” indicator should be green if the lock-in amplifier of the detection module is connected correctly.*

6. Move the stage and optimize the focus to find an area containing the xylem cells of wood samples or herbaceous samples in the bright-field mode.
7. Set the scanning speed at 4.0-16 μs per pixel. Set the image size as 512 × 512 pixels. Check the AL1 checkboxes to activate the SRS channel. Deactivate other channels.
8. Begin scanning by clicking the “XY Repeat”. Finely adjust the *X*, *Y*, and *Z* axes to focus on the area of interest.

**Note: If there is no signal, increase the laser power and adjust the “Phase” and “Gain” in the control software of the detection module to achieve the best contrast of SRS images.*

9. Check the “Kalman” checkbox in the “Filter Mode”. Type in five for the line average. Click the “XY” button to start SRS imaging. Save the image to a file path.

**Note: Do not move the microscope stage.*

10. Repeat Steps h (6-9) for imaging of different views.
11. Repeat Steps h (6-10) for different samples.

(i) Collecting SRS images of cellulose

1. Set the wavelength of the pump beam at 926.5 nm by ticking the “Set Signal”. The frequency difference of the pump and the Stokes beams is now at 1100 cm^{-1}, matching the C-O stretching vibration frequency of the polysaccharides.
2. Repeat Steps h (2-9) for imaging of different views.
3. Repeat Steps i (1-3) for different samples.

(j) Collecting SRS images of lipid / suberin

1. Set the wavelength of the pump beam at 797.2 nm by ticking “Set Signal”. The frequency difference of the pump and the Stokes beams is now at 2850 cm^{-1}, matching the C-H stretching vibration frequency of the polysaccharides.
2. Repeat Steps h (2-9) for imaging of different views.
3. Repeat Steps j (1-3) for different samples.

Quantitative analysis using SRS

Timing: 10 min of setup, 0.5–1 h of unattended computation (depending on the number of measurements), 30 min of quality control, and 0.5–1 h of image processing.

1. Add folders to the Fiji path (using ‘File/Set Path/Add Folder’ from the Fiji menu). New empty folders are used to save the output results.
2. Intensity analyses for specific types of the cell wall can be performed in Fiji software. Open the selected picture and change the image to 8 bit (Fig.6a).
3. Press “Analyze” and “Histogram” to calculate the average photon counts for all measurements (Fig. 6b).
4. Press the list, and the intensity values and counts will be shown (Fig.6c, d).
5. The total intensity values will be divided into 256 parts. From the 0 to 255 value, the intensity counts will be calculated for every tenth value. Then the ratio of the intensity value will be obtained by dividing the sum of ten counts by the total counts.
6. For each type of plant sample, at least three images were selected for intensity analysis. Lignin (1600 cm^{-1}) signals in each pixel are plotted, respectively, as intensity histograms and normalized by total intensity for better comparison.

Potential Experimental Pitfalls

1. Poor spectral resolution of the CRS spectrum. This may be due to the sections of the sample are too thick, or the slit is too wide. Therefore, make sure the sections are ≤10 μm thick and that the slit opening is ≥50 μm.
2. Too much fluorescence of background or other fluorescence interference. To prevent this, be sure to use new coverslips or prepare a new sample for imaging, the samples are not damaged or with bubbles. Additionally, the sections of the samples can be immersed in 75% ethanol before spreading onto the slide, avoiding the chloroplast auto-fluorescence.
3. Sample burns. The sections of the samples were embedded in LR White resin, too thin or laser intensity is too high. Both herbaceous and woody samples should be prepared from fresh or dry plant material but not embedded. Also, the laser intensity should be sufficiently high to obtain good counts per molecule (CPM), to ensure a good signal-to-noise ratio, but also sufficiently low to avoid photobleaching.

Results And Discussion

Sample preparation

Various plant cell wall imaging methods have been developed, revealing details of the cell wall structure and chemical composition, as well as providing information that has proven valuable in the exploitation of biomass polymers [15,35,36]. However, sectioning the stem tissue is the first step in visualization of cell walls by these techniques, which have some significant shortcomings: (i) cumbersome sample preparation and difficulty of sample isolation when small cell wall areas or single cell layers are of interest, since they have to be carefully excised; (ii) damage to samples caused by chemical treatment and photobleaching during fluorescence observation [36]. For example, FTIR spectroscopy is perturbed by the strong infrared absorption of water and, thus, requires the samples to be dried [37]. Except vibratome, cryo-sectioning microtome [38,39]. In our work, various fresh plant materials were prepared and micro cutting sections were obtained with conventional microtechniques by Sliding microtome (Fig.2), allowing us to achieve better data quality by generating sections of equal thickness, which helps to produce sharp images and significantly reduces the risk of reporting inaccurate differences between samples. A suitable microtome should be selected based on the characteristics of the sample, and the sections of the sample can be immersed in 75% ethanol before spreading onto the slide for removing chlorophyll (Table 1). Compared to embedding specimens in resin, this method has the advantage of keeping the tissues alive and reducing sample manipulation, as well as saving time.

CRS image of cell wall at the macroscopic-scale

Cell wall composition is particularly important in plants grown for forage, biofuels, and biomaterials (i.e. wood for construction). In our previous study, we investigated the cytological characteristics and chemical composition of lipid of suberin in endodermal cells during the process of Casparian strip formation using SRS imaging in maize primary roots, suggesting that SRS microscopy is a promising, reliable, and quantitative method to perform noninvasive, label-free imaging of Casparian strips *in vivo*

under physiological conditions [40]. CARS has also been used to gauge the chemical and structural composition in cell walls of birch (*Betula platyphylla*), oak (*Quercus palustris*), and spruce (*Picea asperata*) samples [41].

Here, to further collect CARS and SRS images of cell walls, we followed the experimental schematic (Fig.1d) and set the wavelength of the pump beam, frequency difference of the pump and the Stokes beams (Fig.2). The cross-sections were observed using CRS microscopy and were acquired at 1600 cm^{-1} (C-C), 1100 cm^{-1}(C-O), 2805 cm^{-1} (C-H), respectively (Fig.3). CARS image of lignin, cellulose and lipid in *Populus* were investigated (Fig. 4a-c). In addition, SRS images of lignin in the xylem cell wall of *Arabidopsis* root and stem (Fig. 3d,e). Moreover, Casparian strips form a network in the primary walls of the endodermal cell, here, lignin and lipid of suberin in Casparian strips of maize root were also imaged by SRS, indicating that the development progress of Casparian strips (Fig.4f). The cytological characteristics and lignin, cellulose and lipid of cell walls in stem of *Bruguiera sexangula* were also investigated, which were salt-tolerant plants (Fig.4g-l). Besides these images of local area, the large scale of SRS images was also showed in Fig. 4l. Interestingly, the higher-magnification and 3D surface plots of cell wall SRS image in *Populus* (Fig.5) showed that, the lignin distribution of large vessel cell appears to be different and mainly in the cell Corner (Fig. 5d), the cellulose content were evenly distributed in primary cell wall and middle lamella (Fig.5e), and the lipid signals were mainly obtained in primary cell wall(Fig.5f). Additionally, some troubleshooting needed to be pay more attention. Such as made sure the intensity of the laser at the sample position is correct, and increased laser power accordingly (Table 1). The ability to characterize *in situ* molecular vibrations has created exciting new opportunities for cell wall imaging. Notably, compared to traditional Raman methods, CRS has been used to analyze substances that are difficult to label, such as polysaccharides and large biomolecules, including lignin, achieving higher orders of resolution and better sensitivity. This protocol offers researchers a more comprehensive result using simplified methods with label-free, fast and high-specificity altogether.

This protocol uses CRS approaches, including CARS and SRS, which are effective methods for imaging complex chemistry based on molecular vibrations in biological molecules. CRS microscopy has been extensively applied to detect the distribution and quantify the cell wall composition [19,40-42]. Although CARS microscopy offers label-free chemical imaging with high sensitivity and high spatial resolution, its signal also suffers from a non-resonant electronic background component that can, to a certain degree, distort the chemical information of interest, making quantitative image interpretation challenging. In addition, SRS back signal detection is still a technical problem, and considerable engineering efforts will be needed to achieve a better solution. Other long-term goals in the further optimization of unlabeled imaging technology include how to further distinguish different chemical components, especially how to better use the Raman peak molecular characteristics to observe the dynamic distribution and behavior of specific molecules in living cells.

SRS c**omputational analysisof cell wall composition**

SRS is another label-free imaging method and the most promising techniques for imaging chemical bonds based on the photo-switching concept of stimulated emission depletion [43,44]. In our previous study, we examined the effects of the microRNA miR857, which is involved in the regulation of lignin content and consequently morphogenesis of the secondary xylem. The intensity of the lignin signals among wild-type, lignin-deficient lines (overexpressing *35S:MIR857*), and lignin-overproducing (*mir857* mutant) plants in *Arabidopsis thaliana* were analyzed by SRS [42]. In addition, compared with images stained using the traditional chemical dye FY 088, SRS images at the CH_2 stretching vibration show a higher sensitivity and specificity for the lipid component of suberin lamellae, especially with respect to the latent capacity of SRS images to acquire a signal for a low-abundance substance in the primary site of suberin appearance without a non-resonant background [40]. To further analysis of the distribution of chemical components in cell walls in woody plants, SRS quantitative and straightforward image analysis were showed in Fig. 6. Here, as the lignin content for example, we analyzed the intensity of the lignin signals among wild-type, lignin-overproducing lines (overexpressing *35S:MIR408*), and then used image analysis software such as Fiji or ImageJ to calculate fluorescence intensity of the cell wall in the secondary xylem. Individual cells were manually selected from SRS image acquisitions, in combination with further image analysis steps. Intensity analyses for specific types of cell wall samples can be computed as described. The fluorescence intensity of the cell wall in the secondary xylem is lower and more narrowly distributed in *Populus* plants overexpressing *35S:MIR408* than in the wild type with an intensity profile (Fig.7), as well as the lignin content. Although Chemical imaging of poplar wood cell walls were investigated by confocal Raman microscopy [6,45], the quantitative analysis of which was difficult and challenge. Compared to CRM, SRS microscopy is free of non-resonant background and linearly dependent on the analyte concentration, thus offering quantitative and straightforward image analysis [34]. These results confirmed that our CRS images of the cell wall can be used for further analysis of chemical composition, which was a superior alternative for fast and large-area biological chemical imaging in biology.

Conclusions

In summary, this cell wall imaging technique can detect specific chemical bonds within particular molecules, which was applicable to real-time *in situ* quantification in plant tissues with high chemical specificity and spatial resolution. Therefore, CRS overcame the limitations of existing techniques and offered remarkable new insights into the mechanisms of plant biology by nondestructively gathering spatially resolved chemical information and enabling quantitative microanalysis of chemical compositions of plant cell walls, which can be widely used in plant cell research, pulp industry and biofuel analysis.

Declarations

Ethics approval and consent to participate

Not applicable.

Consent for publication

Not applicable.

Availability of data and materials

All data generated or analyzed during this study are included in this published article.

Competing interests

The authors declare that they have no competing interests.

Funding

This work is supported by the National Natural Science Foundation of China (31800504), and the China Postdoctoral Science Foundation (2018M631246, 2018M641096).

Authors' contributions

HMX performed the experiments and analysis, and wrote the paper. HMX wrote the protocol with the help of YYZ and YZS tested the protocol and helped in writing the software manuals. YYG and YM provided the experimental materials. XQH and YPJ edited and revised the paper. JXL designed the experiment and revised the paper.

Acknowledgments

The authors thank Professor Xiaoliang Sunney Xie, Yanyi Huang at Peking University for technical support of CRS microscope and Tobias Grunske at APE GmbH for providing technical information of the APE PicoEmerald laser.

References

1. Saar BG, Zeng Y, Freudiger CW, Liu YS, Himmel ME, Xie XS, et al. Label-free, real-time monitoring of biomass processing with stimulated Raman scattering microscopy. Angewandte Chemie. 2010;49:5476-9.
2. Sarkar P, Bosneaga E, Auer M. Plant cell walls throughout evolution: towards a molecular understanding of their design principles. Journal of experimental botany. 2009;60:3615-35.
3. Zeng YN, Himmel ME, Ding SY. Visualizing chemical functionality in plant cell walls. Biotechnology for biofuels. 2017;10:
4. Ding SY, Himmel ME. The maize primary cell wall microfibril: A new model derived from direct visualization. Journal of Agricultural and Food Chemistry. 2006;54:597-606.
5. Lee KJD, Marcus SE, Knox JP. Cell Wall Biology: Perspectives from Cell Wall Imaging. Molecular plant. 2011;4:212-19.

6. Gierlinger N, Keplinger T, Harrington M. Imaging of plant cell walls by confocal Raman microscopy. Nature protocols. 2012;7:1694-708.
7. Pettolino FA, Walsh C, Fincher GB, Bacic A. Determining the polysaccharide composition of plant cell walls. Nature protocols. 2012;7:1590-607.
8. Voiniciuc C, Pauly M, Usadel B. Monitoring polysaccharide dynamics in the plant cell wall. Plant physiology. 2018;176:2590-600.
9. Soukup A. Selected simple methods of plant cell wall histochemistry and staining for light microscopy. Methods in molecular biology. 2014;1080:25-40.
10. Baskin TI, Beemster GT, Judy-March JE, Marga F. Disorganization of cortical microtubules stimulates tangential expansion and reduces the uniformity of cellulose microfibril alignment among cells in the root of *Arabidopsis*. Plant physiology. 2004;135:2279-90.
11. Fromm J, Rockel B, Lautner S, Windeisen E, Wanner G. Lignin distribution in wood cell walls determined by TEM and backscattered SEM techniques. Journal of Structural Biology. 2003;143:77-84.
12. Freudiger CW, Min W, Saar BG, Lu S, Holtom GR, He CW, et al. Label-free biomedical imaging with high sensitivity by Stimulated Raman Scattering Microscopy. Science. 2008;322:1857-61.
13. Verhertbruggen Y, Marcus SE, Haeger A, Verhoef R, Schols HA, McCleary BV, et al. Developmental complexity of arabinan polysaccharides and their processing in plant cell walls. Plant Journal. 2009;59:413-25.
14. Sun L, Simmons BA, Singh S. Understanding Tissue specific compositions of bioenergy feedstocks through hyperspectral Raman Imaging. Biotechnology and bioengineering. 2011;108:286-95.
15. Clausen MH, Willats WG, Knox JP. Synthetic methyl hexagalacturonate hapten inhibitors of anti-homogalacturonan monoclonal antibodies LM7, JIM5 and JIM7. Carbohydr Res. 2003;338:1797-800.
16. Herve C, Marcus SE, Knox JP. Monoclonal antibodies, carbohydrate-binding modules, and the detection of polysaccharides in plant cell walls. Methods in molecular biology. 2011;715:103-13.
17. Tobimatsu Y, Wagner A, Donaldson L, Mitra P, Niculaes C, Dima O, et al. Visualization of plant cell wall lignification using fluorescence-tagged monolignols. Plant Journal. 2013;76:357-66.
18. Ovecka M, Vaskebova L, Komis G, Luptovciak I, Smertenko A, Samaj J. Preparation of plants for developmental and cellular imaging by light-sheet microscopy. Nature protocols. 2015;10:1234-47.
19. Zhao YY, Man Y, Wen JL, Guo YY, Lin JX. Advances in imaging plant cell walls. Trends in plant science. 2019;24:867-78.
20. Kirby AR. Atomic force microscopy of plant cell walls. Methods in molecular biology. 2011;715:169-78.
21. Peaucelle A. AFM-based mapping of the elastic properties of cell walls: at tissue, cellular, and subcellular resolutions. Jove-J Vis Exp. 2014;

22. Zhang T, Zheng YZ, Cosgrove DJ. Spatial organization of cellulose microfibrils and matrix polysaccharides in primary plant cell walls as imaged by multichannel atomic force microscopy. Plant Journal. 2016;85:179-92.
23. Yang HY, Yang SN, Kong JL, Dong AC, Yu SN. Obtaining information about protein secondary structures in aqueous solution using Fourier transform IR spectroscopy. Nature protocols. 2015;10:
24. Gierlinger N, Schwanninger M. Chemical imaging of poplar wood cell walls by confocal Raman microscopy. Plant physiology. 2006;140:1246-54.
25. Gierlinger N, Sapei L, Paris O. Insights into the chemical composition of Equisetum hyemale by high resolution Raman imaging. Planta. 2008;227:969-80.
26. Song CW, Shen WW, Du L, Wen JL, Lin JX, Li RL. Development and chemical characterization of Casparian strips in the roots of Chinese fir (*Cunninghamia lanceolata*). Trees-Struct Funct. 2019;33:827-36.
27. Nan XL, Cheng JX, Xie XS. Vibrational imaging of lipid droplets in live fibroblast cells with coherent anti-Stokes Raman scattering microscopy. J Lipid Res. 2003;44:2202-08.
28. Li JF, Tian XD, Li SB, Anema JR, Yang ZL, Ding Y, et al. Surface analysis using shell-isolated nanoparticle-enhanced Raman spectroscopy. Nature protocols. 2013;8:52-65.
29. Volkmer A, Cheng JX, Xie XS. Vibrational imaging with high sensitivity via epidetected coherent anti-Stokes Raman scattering microscopy. Phys Rev Lett. 2001;87:
30. Saar BG, Freudiger CW, Reichman J, Stanley CM, Holtom GR, Xie XS. Video-Rate Molecular Imaging in Vivo with Stimulated Raman Scattering. Science. 2010;330:1368-70.
31. Min W, Freudiger CW, Lu SJ, Xie XS. Coherent Nonlinear Optical Imaging: Beyond Fluorescence Microscopy. Annual Review of Physical Chemistry, Vol 62. 2011;62:507-30.
32. Fu D, Lu FK, Zhang X, Freudiger C, Pernik DR, Holtom G, et al. Quantitative chemical imaging with multiplex Stimulated Raman Scattering Microscopy. J Am Chem Soc. 2012;134:3623-26.
33. Weeks T, Schie I, den Hartigh LJ, Rutledge JC, Huser T. Lipid-cell interactions in human monocytes investigated by doubly-resonant coherent anti-Stokes Raman scattering microscopy. Journal of biomedical optics. 2011;16:
34. Hu FH, Shi LX, Min W. Biological imaging of chemical bonds by stimulated Raman scattering microscopy. Nature Methods. 2019;16:830-42.
35. McCartney L, Marcus SE, Knox JP. Monoclonal antibodies to plant cell wall xylans and arabinoxylans. J Histochem Cytochem. 2005;53:543-6.
36. Lee KJ, Knox JP. Resin embedding, sectioning, and immunocytochemical analyses of plant cell walls in hard tissues. Methods in molecular biology. 2014;1080:41-52.
37. Gorzsas A, Stenlund H, Persson P, Trygg J, Sundberg B. Cell-specific chemotyping and multivariate imaging by combined FT-IR microspectroscopy and orthogonal projections to latent structures (OPLS) analysis reveals the chemical landscape of secondary xylem. The Plant journal : for cell and molecular biology. 2011;66:903-14.

38. Pradhan Mitra P, Loque D. Histochemical staining of Arabidopsis thaliana secondary cell wall elements. J Vis Exp. 2014;
39. Gierlinger N, Keplinger T, Harrington M. Imaging of plant cell walls by confocal Raman microscopy. Nature protocols. 2012;7:1694-708.
40. Man Y, Zhao YY, Ye R, Lin JX, Jing YP. In vivo cytological and chemical analysis of Casparian strips using stimulated Raman scattering microscopy. Journal of plant physiology. 2018;220:136-44.
41. Pohling C, Brackmann C, Duarte A, Buckup T, Enejder A, Motzkus M. Chemical imaging of lignocellulosic biomass by CARS microscopy. Journal of Biophotonics. 2014;7:126-34.
42. Zhao YY, Lin S, Qiu ZB, Cao DC, Wen JL, Deng X, et al. MicroRNA857 is involved in the regulation of secondary growth of vascular tissues in *Arabidopsis*. Plant physiology. 2015;169:2539-52.
43. Cheng JX, Xie XS. Vibrational spectroscopic imaging of living systems: An emerging platform for biology and medicine. Science. 2015;350:
44. Prince RC, Frontiera RR, Potma EO. Stimulated Raman Scattering: From Bulk to Nano. Chem Rev. 2017;117:5070-94.
45. Gierlinger N, Schwanninger M. Chemical imaging of poplar wood cell walls by confocal Raman microscopy. Plant physiology. 2006;140:1246-54.

Tables

Table 1 | The problems and solution methods during the protocol

Number	Problem	Possible reason	Solution
1	A lack of good contiguous microsections	An inappropriate microtome was used	A suitable microtome should be selected based on the characteristics of the sample
2	Intensity is too low	Laser intensity is too low	Make sure the intensity of the laser at the sample position is correct; increase laser power accordingly
		Exposure time is insufficient	Increase the exposure time
		Samples are overtreated and not suitable for imaging	Prepare the samples carefully according to step 1
3	Poor spectral resolution of the CRS spectrum	The sections of the sample are too thick, or the slit is too wide	Make sure the sections are ≤10 μm thick and that the slit opening is ³50 μm
4	Too much fluorescence of background	Coverslips are dirty, there are bubbles, or the samples are damaged	Use new coverslips or prepare a new sample for imaging
5	Other fluorescence interference	Chloroplast auto-fluorescence	The sections of the sample can be immersed in 75% ethanol before spreading onto the slide
6	Sample burns	The sections of the sample were embedded in LR White resin or laser intensity is too high.	Both herbaceous and woody samples should be prepared from fresh or dry plant material but not embedded The laser intensity should be sufficiently high to obtain good counts per molecule (CPM), to ensure a good signal-to-noise ratio, but also sufficiently low to avoid photobleaching

Figures

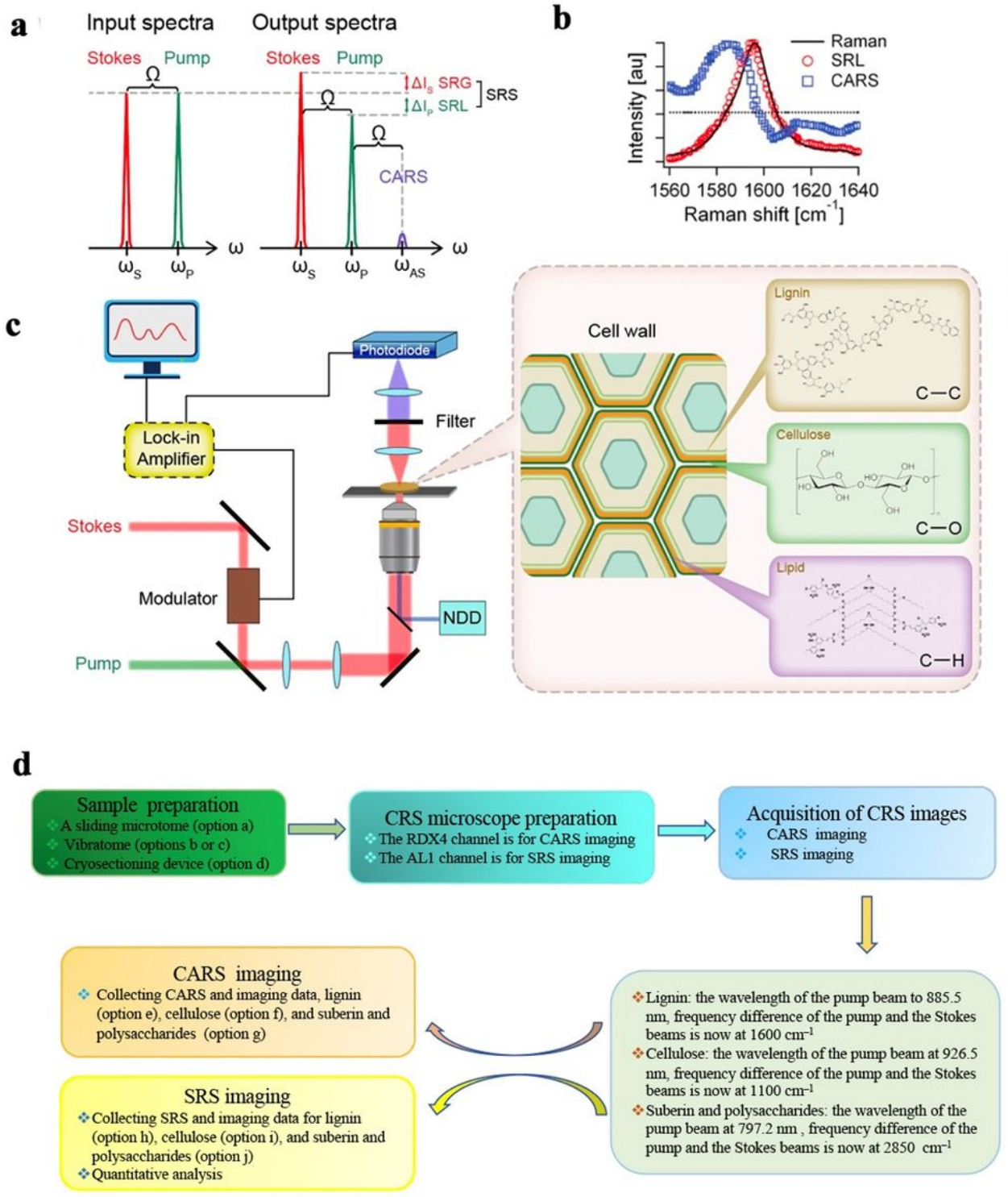

Figure 1

Principle and design of CRS microscopy. Modified from Freudiger et al. (2008)24. CRS microscopy mainly includes two sub-types, coherent anti-Stokes Raman scattering (CARS) microscopy and stimulated Raman scattering (SRS) microscopy, both of which can be performed by setting the wavelength of the pump beam in a single setup. (a) The principle of SRS microscopy. Two input beams (Stokes and Pump) are focused on the sample; when the difference in energy between the two beams (Ω) matches that of a

specific chemical bond in the sample, then an additional signal is produced. Input and output spectra of SRS and CARS. SRS leads to an intensity increase in the Stokes beam (SRG) and an intensity decrease in the pump beam (SRL). Also shown (not to scale) is the CARS signal generated at the anti-Stokes frequency ωAS when the energy difference between the pump beam photon and the Stokes beam photon matches the vibrational frequency (Ωvib) of a specific chemical bond. (b) Agreement of SRL spectrum (red circles) with the spontaneous Raman spectrum (black line) of the Raman peak (1595 cm-1) of 10 mM retinol in ethanol. The distorted CARS spectrum (blue squares) exhibits a typical peak shift, dispersive shape, and non-resonant background. (c) Plant cell wall imaging of the chemical composition of stem and roots. CRS microscope with forward and epi detection. The Stokes beam is modulated by an electro-optic modulator. The transmitted or reflected pump beam is filtered and detected by a large-area photodiode (PD). The SRL is measured by a lock-in amplifier to provide a pixel of the image. The CARS signal detected by the NDD. (d) Schematic of the CRS images of plant cell wall composition.

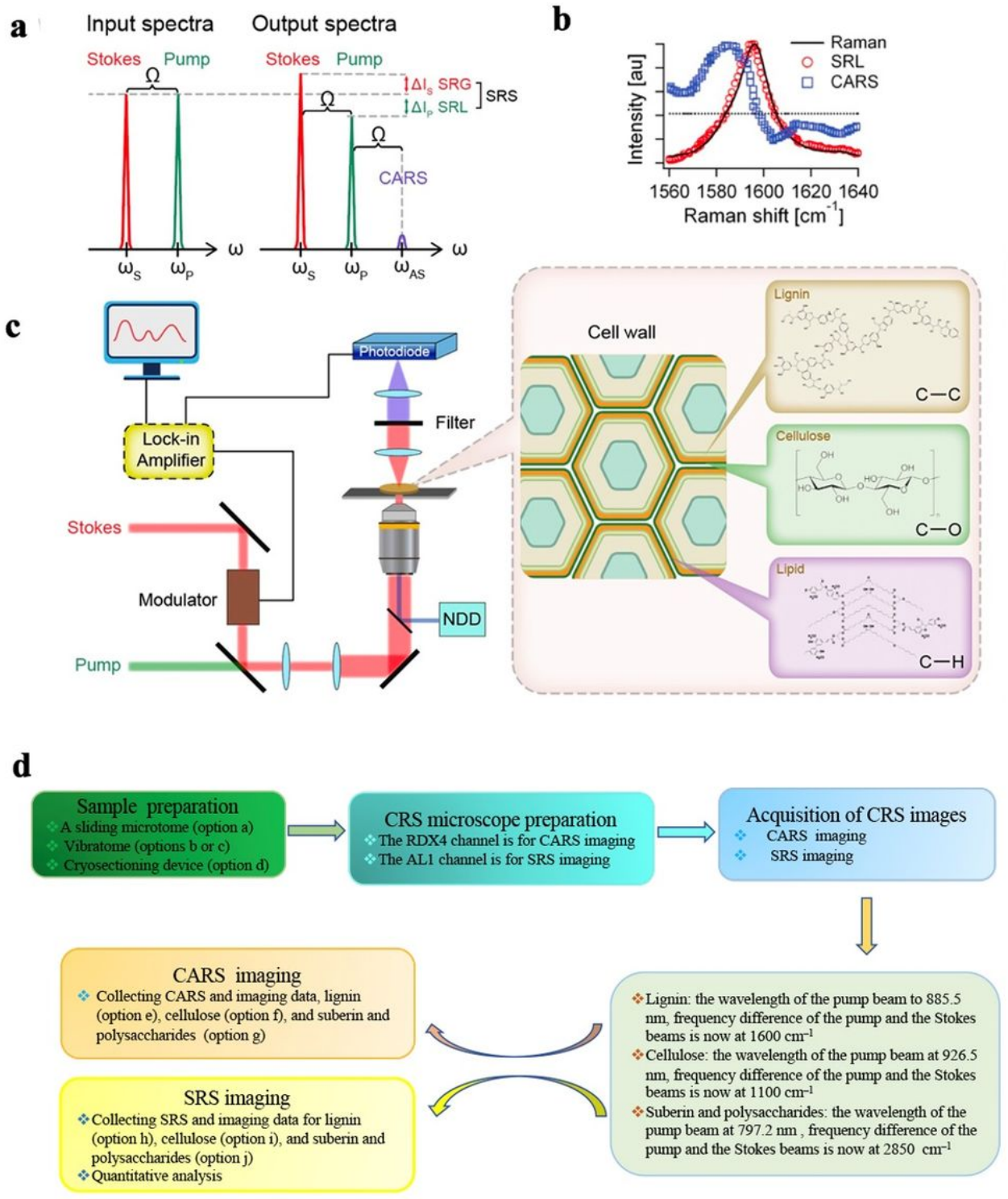

Figure 1

Principle and design of CRS microscopy. Modified from Freudiger et al. (2008)24. CRS microscopy mainly includes two sub-types, coherent anti-Stokes Raman scattering (CARS) microscopy and stimulated Raman scattering (SRS) microscopy, both of which can be performed by setting the wavelength of the pump beam in a single setup. (a) The principle of SRS microscopy. Two input beams (Stokes and Pump) are focused on the sample; when the difference in energy between the two beams (Ω) matches that of a

specific chemical bond in the sample, then an additional signal is produced. Input and output spectra of SRS and CARS. SRS leads to an intensity increase in the Stokes beam (SRG) and an intensity decrease in the pump beam (SRL). Also shown (not to scale) is the CARS signal generated at the anti-Stokes frequency ωAS when the energy difference between the pump beam photon and the Stokes beam photon matches the vibrational frequency (Ωvib) of a specific chemical bond. (b) Agreement of SRL spectrum (red circles) with the spontaneous Raman spectrum (black line) of the Raman peak (1595 cm-1) of 10 mM retinol in ethanol. The distorted CARS spectrum (blue squares) exhibits a typical peak shift, dispersive shape, and non-resonant background. (c) Plant cell wall imaging of the chemical composition of stem and roots. CRS microscope with forward and epi detection. The Stokes beam is modulated by an electro-optic modulator. The transmitted or reflected pump beam is filtered and detected by a large-area photodiode (PD). The SRL is measured by a lock-in amplifier to provide a pixel of the image. The CARS signal detected by the NDD. (d) Schematic of the CRS images of plant cell wall composition.

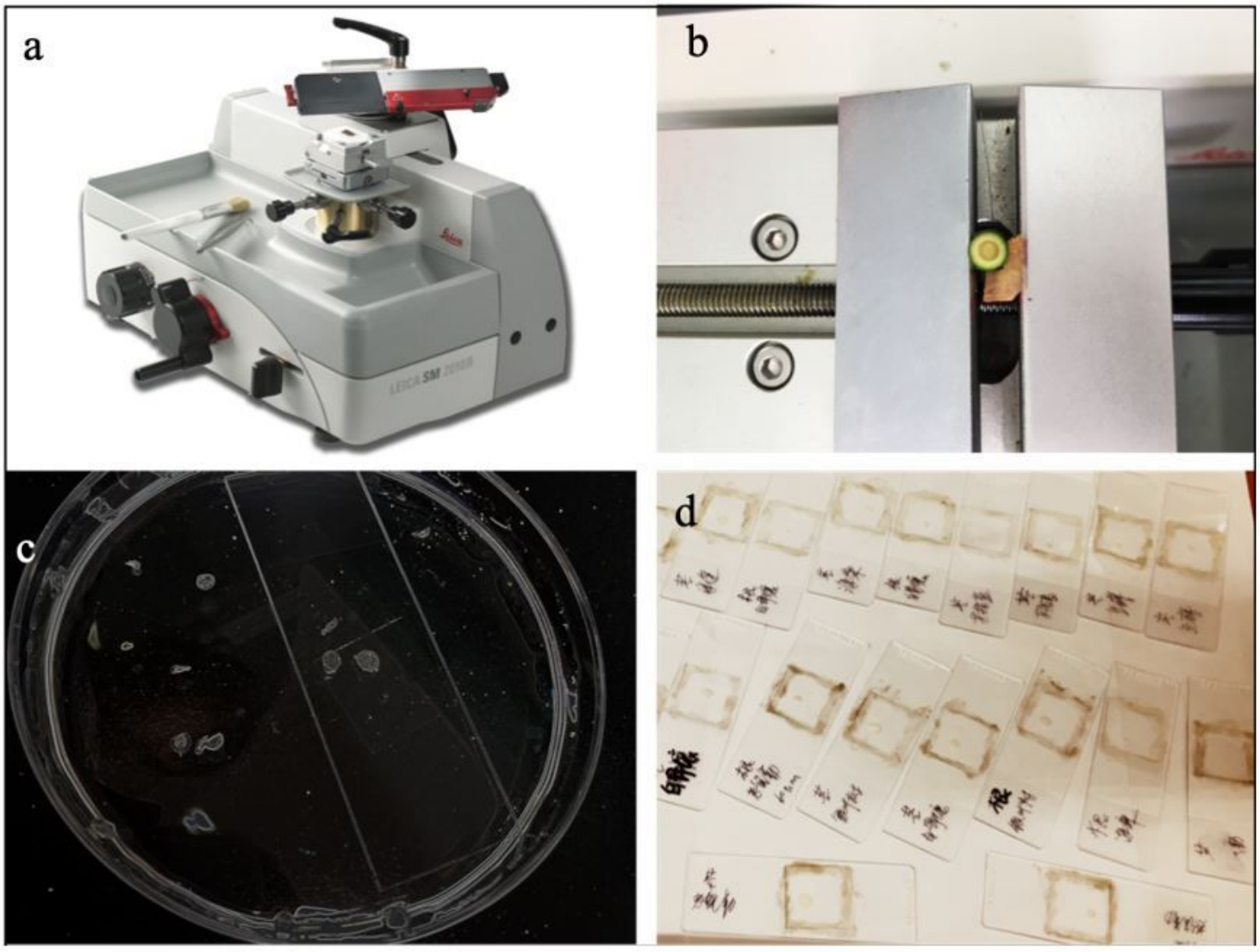

Figure 2

Micro cuttings could be obtained with conventional microtechniques. (a) Sliding microtome. (b) The plant samples are cut into 10-μm-thick slices, and these cross-sections are gently washed using distilled water,

then were transferred from the buffer tray into a glass beaker and then to a clear Petri plate (c). (d) The sections were transferred to the slide and seal the slide.

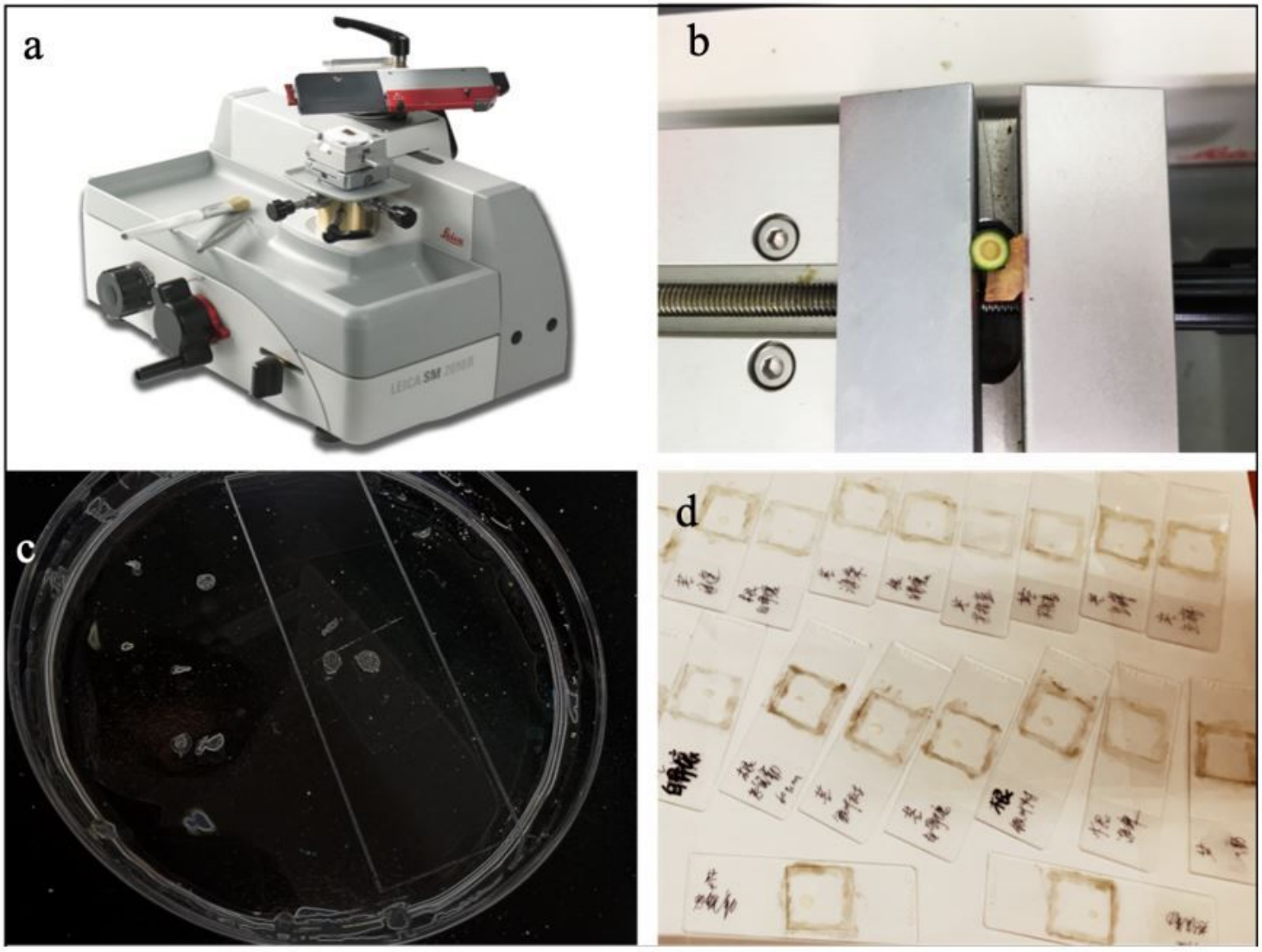

Figure 2

Micro cuttings could be obtained with conventional microtechniques. (a) Sliding microtome. (b) The plant samples are cut into 10-μm-thick slices, and these cross-sections are gently washed using distilled water, then were transferred from the buffer tray into a glass beaker and then to a clear Petri plate (c). (d) The sections were transferred to the slide and seal the slide.

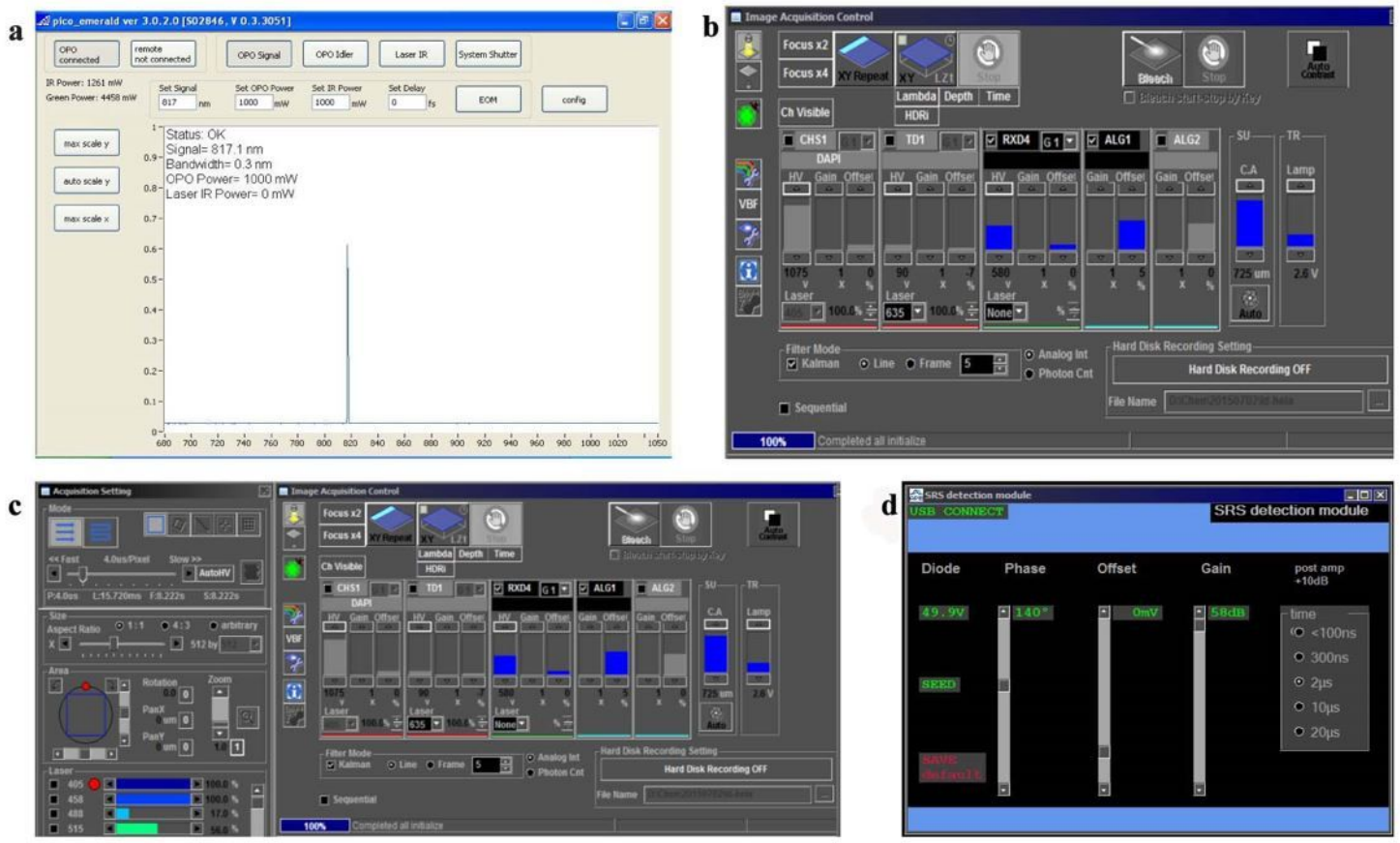

Figure 3

The detection and acquisition of CRS images. (a) Control software setting. Turn on the key switch and power switch of the laser control unit. Then turn on the power switch of the chiller and check whether the water-cooled pipe joint is leaking. Set the temperature at 23°C. Wait about 0.5 h until the temperature has stabilized. (b) Dialog window for detection channel settings. Switch on the panel PC. The control software (picoEmerald ver 3.0.2.0) will start automatically (a). Confirm with YES when the system asks you whether to start the laser. This takes about 0.5 h to warm up and light the laser. (c) Dialog window for image settings. Turn on the main power switch, key switch, scanning module, and motorized translation stage of the microscope. (d) Dialog window for SRS detection settings. Open the FV10-ASW3.0 software of the microscope by double-clicking on the FV10-ASW3.0 icon. The RDX4 channel is for CARS imaging, while the AL1 channel is for SRS imaging.

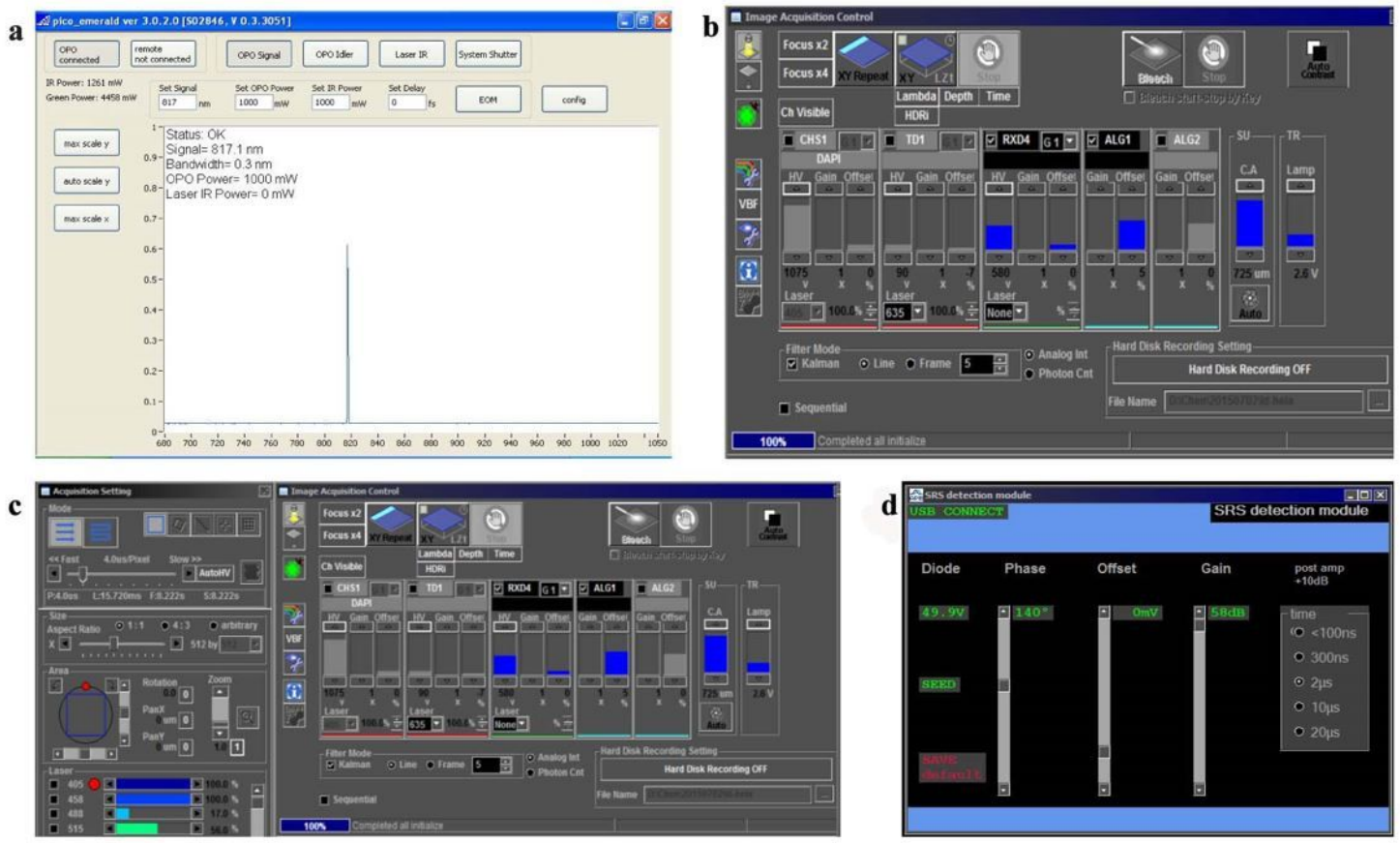

Figure 3

The detection and acquisition of CRS images. (a) Control software setting. Turn on the key switch and power switch of the laser control unit. Then turn on the power switch of the chiller and check whether the water-cooled pipe joint is leaking. Set the temperature at 23°C. Wait about 0.5 h until the temperature has stabilized. (b) Dialog window for detection channel settings. Switch on the panel PC. The control software (picoEmerald ver 3.0.2.0) will start automatically (a). Confirm with YES when the system asks you whether to start the laser. This takes about 0.5 h to warm up and light the laser. (c) Dialog window for image settings. Turn on the main power switch, key switch, scanning module, and motorized translation stage of the microscope. (d) Dialog window for SRS detection settings. Open the FV10-ASW3.0 software of the microscope by double-clicking on the FV10-ASW3.0 icon. The RDX4 channel is for CARS imaging, while the AL1 channel is for SRS imaging.

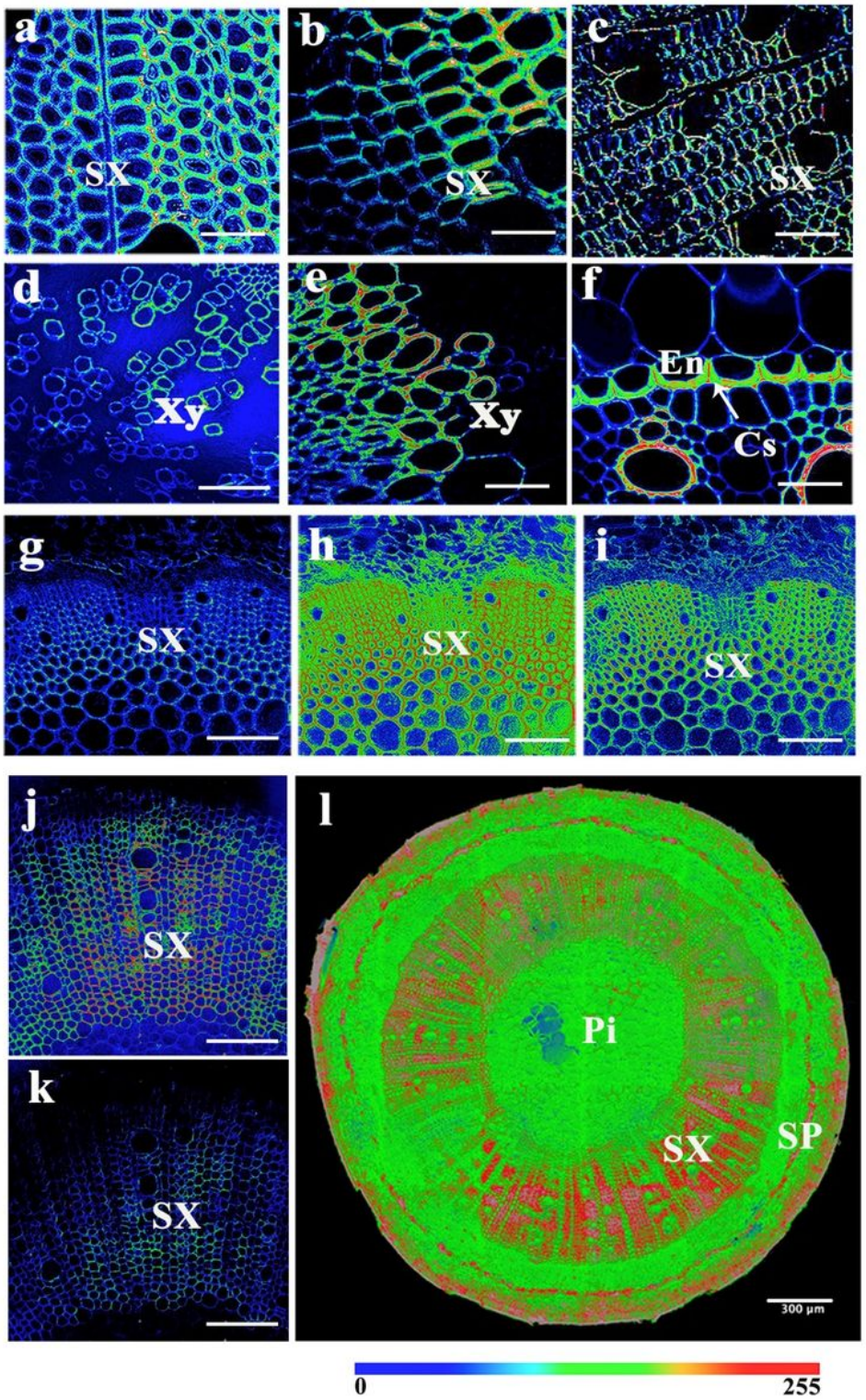

Figure 4

CRS images of the lignin, cellulose and lipid in xylem cell wall. (a-b) CARS image of lignin, cellulose and lipid in Populus. (d-e) SRS images lignin of root xylem and cellulose of stem xylem in Arabidopsis thaliana. (f) SRS images of the cell wall in the Casparian strips of maize root. (g-i) SRS images of lignin, cellulose and lipid in the secondary xylem cell wall of Bruguiera sexangula stem. (j-l) SRS images of

lignin, cellulose and lipid in the secondary xylem cell wall of Derris trifoliata. SX, secondary xylem; Xy, xylem; Cs, Casparian strips; En, endodermis. Scale bars in a-k are 50 μm, and l are 300 μm.

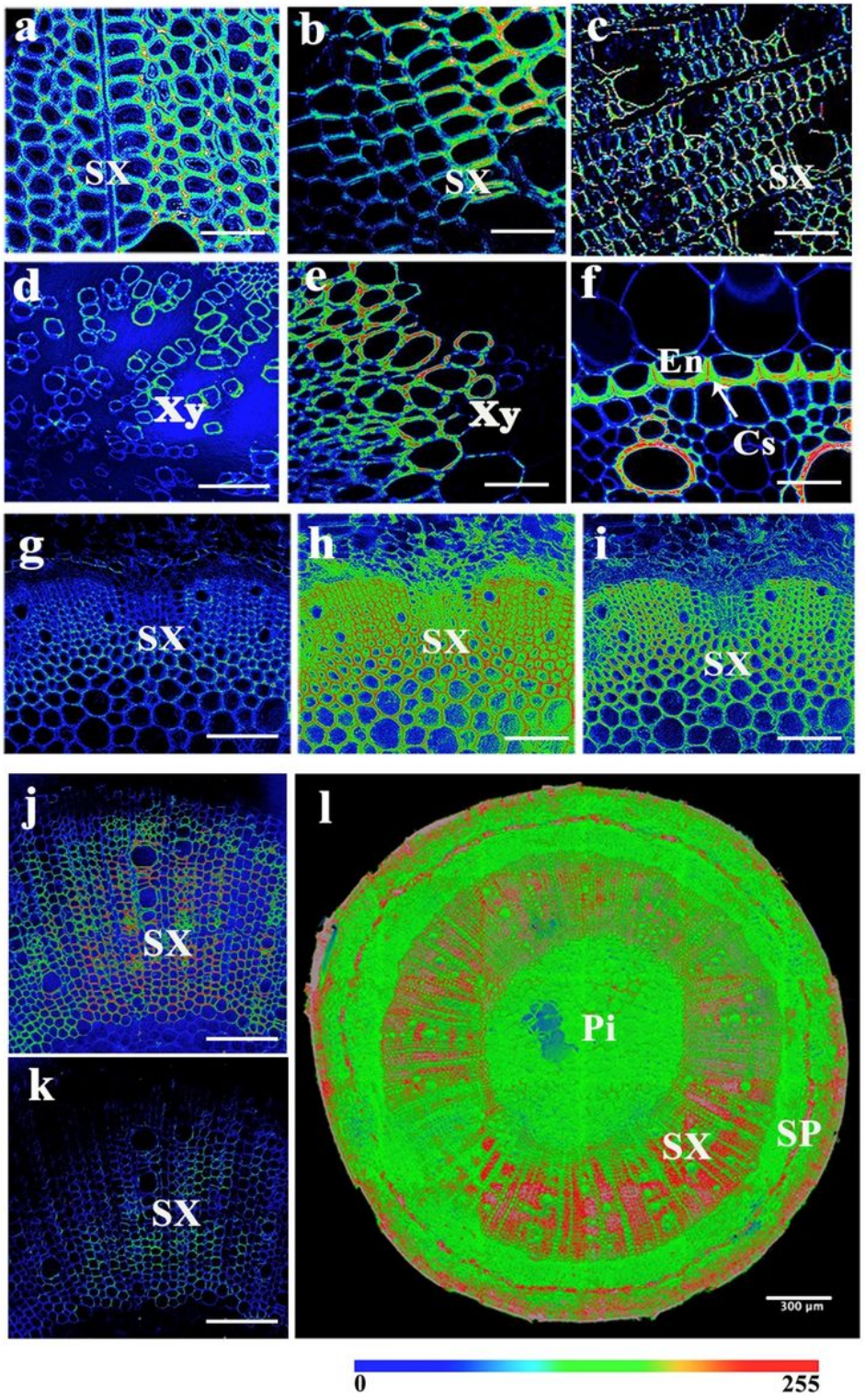

Figure 4

CRS images of the lignin, cellulose and lipid in xylem cell wall. (a-b) CARS image of lignin, cellulose and lipid in Populus. (d-e) SRS images lignin of root xylem and cellulose of stem xylem in Arabidopsis thaliana. (f) SRS images of the cell wall in the Casparian strips of maize root. (g-i) SRS images of lignin,

cellulose and lipid in the secondary xylem cell wall of Bruguiera sexangula stem. (j-l) SRS images of lignin, cellulose and lipid in the secondary xylem cell wall of Derris trifoliata. SX, secondary xylem; Xy, xylem; Cs, Casparian strips; En, endodermis. Scale bars in a-k are 50 μm, and l are 300 μm.

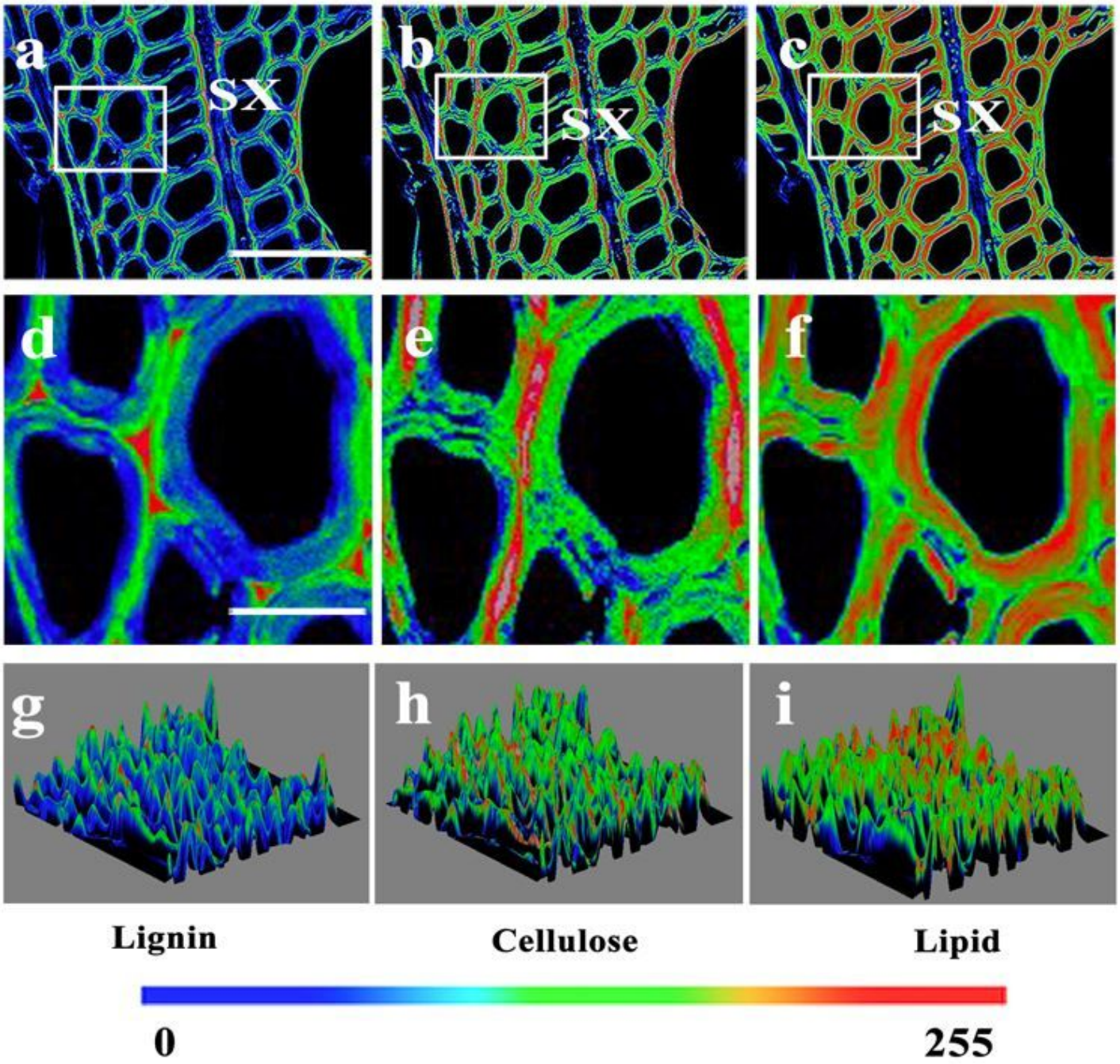

Figure 5

SRS images of the lignin, cellulose and lipid in xylem cell wall. (a-c) SRS images of lignin, cellulose and lipid in the secondary xylem cell wall of Populus. The white boxes show the areas of the cell walls that are magnified in (d), (e), and (f). The 3D surface plots were shown in (g-i). SX, secondary xylem; Scale bars in a-f are 50 μm.

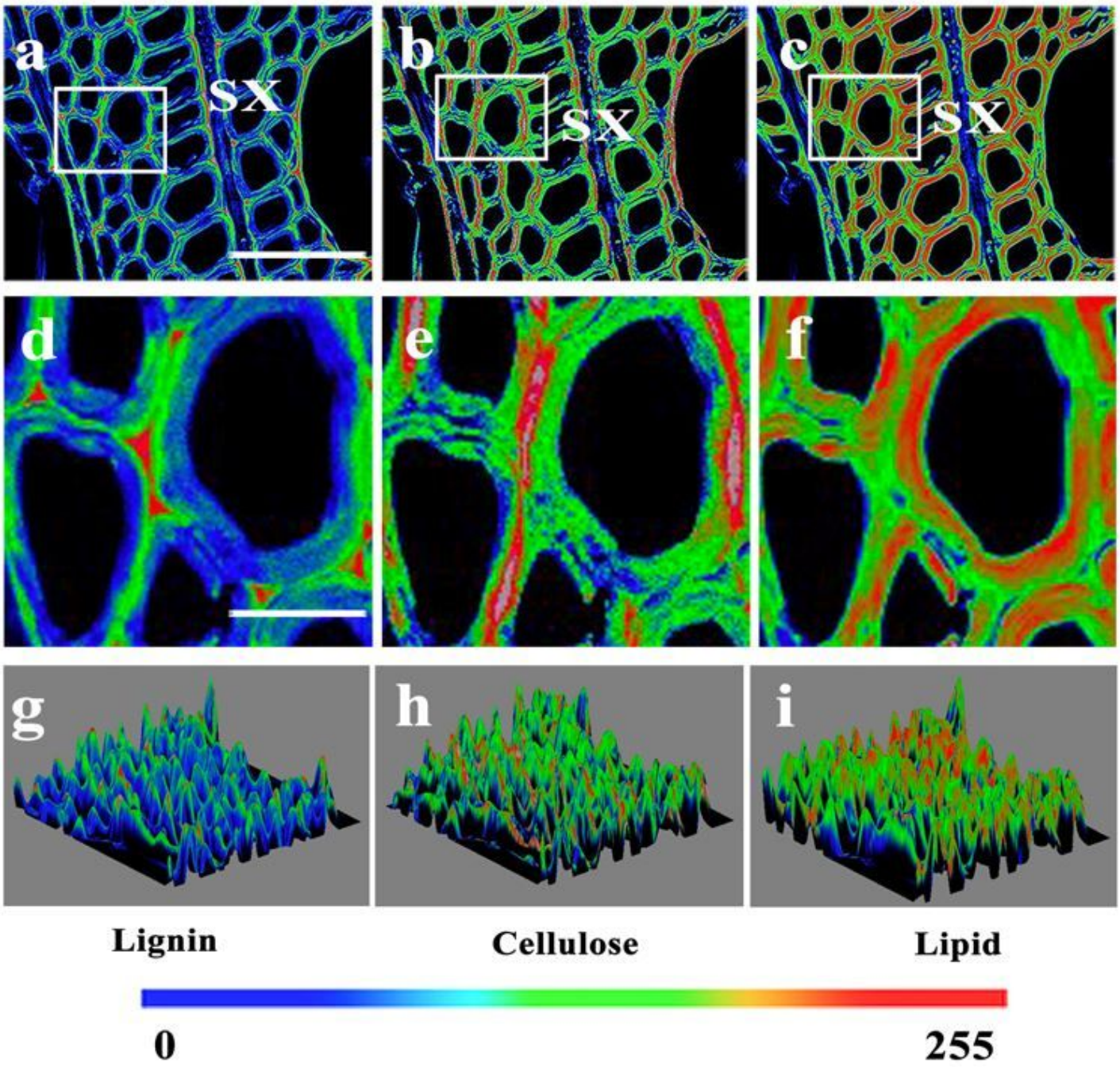

Figure 5

SRS images of the lignin, cellulose and lipid in xylem cell wall. (a-c) SRS images of lignin, cellulose and lipid in the secondary xylem cell wall of Populus. The white boxes show the areas of the cell walls that are magnified in (d), (e), and (f). The 3D surface plots were shown in (g-i). SX, secondary xylem; Scale bars in a-f are 50 μm.

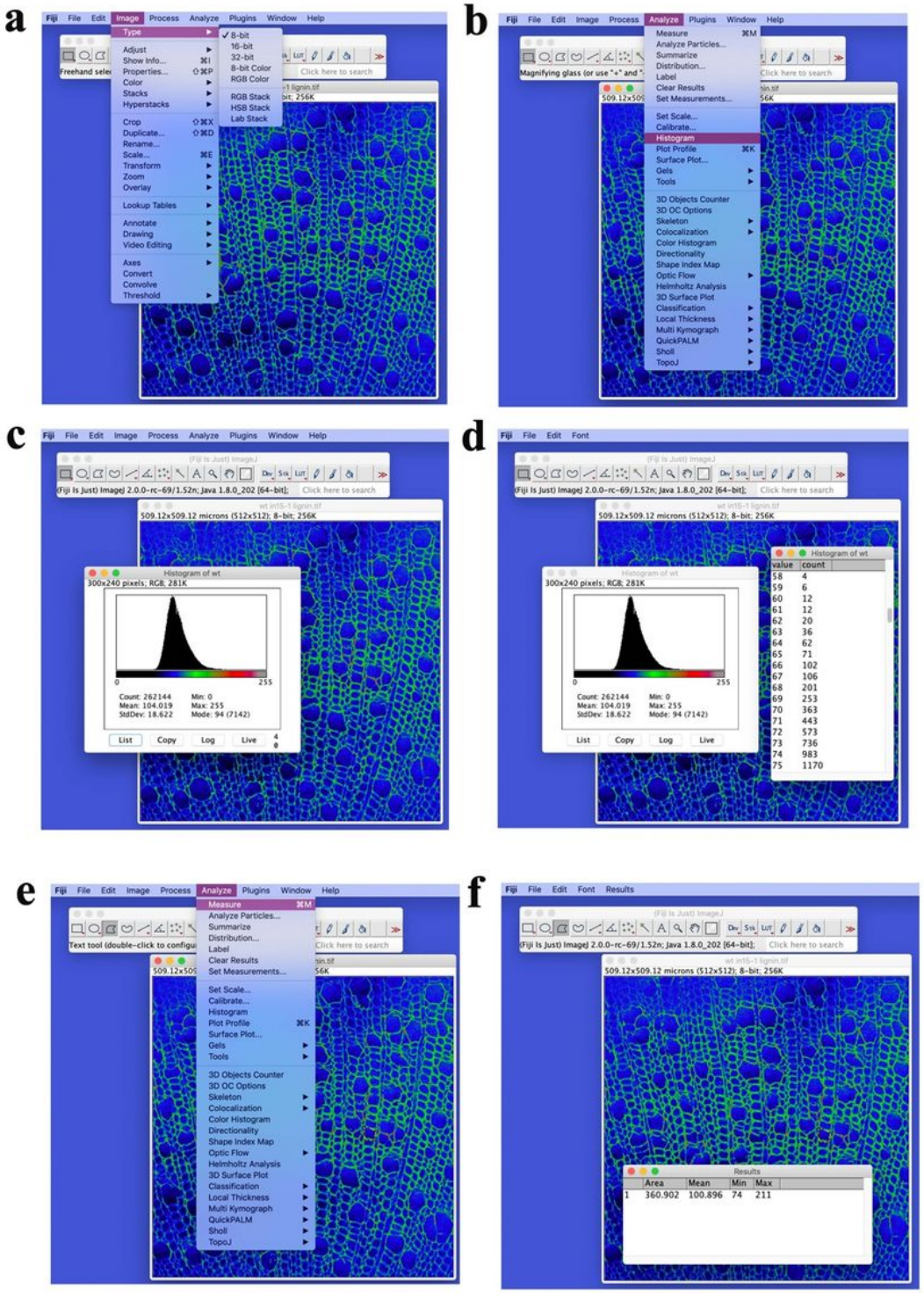

Figure 6

SRS quantitative analysis of lignin in the secondary xylem cell wall in Populus. (a) Image setting. Intensity analyses for specific types of the cell wall can be performed in Fiji software. Open the selected picture and change the image to 8 bit. (b) Calculate the average photon counts for all measurements. Press “Analyze” and “Histogram” to calculate the average photon counts for all measurements. (c) (d) Obtained the ratio of the intensity value. Press the list, and the intensity values and counts will be shown.

The total intensity values will be divided into 256 parts. From the 0 to 255 value, the intensity counts will be calculated for every tenth value. Then the ratio of the intensity value will be obtained by dividing the sum of ten counts by the total counts. (e) (f) Calculate the average intensity for selected cells. For each type of plant sample, at least three images were selected for intensity analysis. About 50 cells were selected for further analysis, press “Analyze” and “Measure” to calculate the average intensity for selected cells. Lignin (1600 cm−1) signals in each pixel are plotted, respectively, as intensity histograms and normalized by total intensity for better comparison.

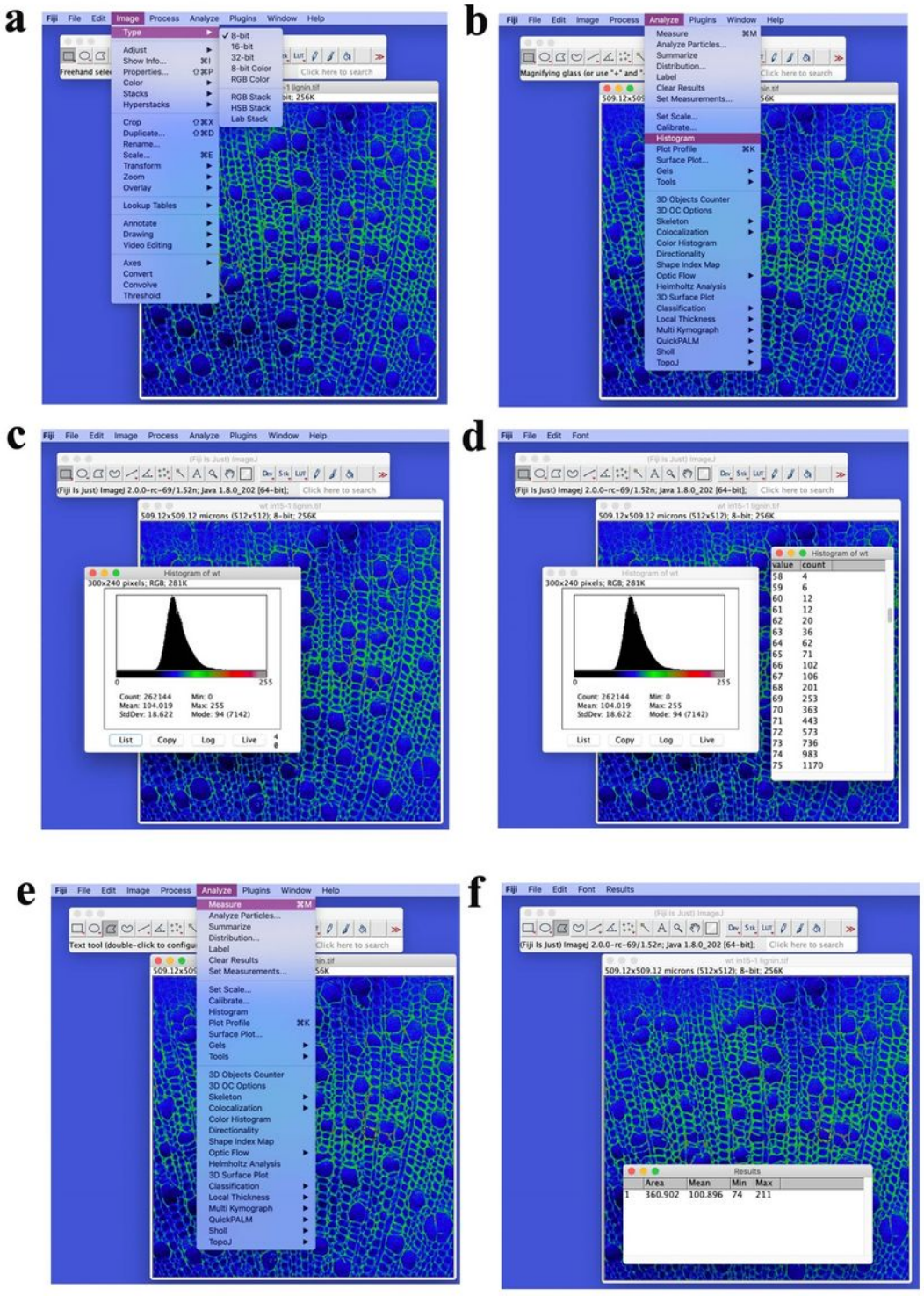

Figure 6

SRS quantitative analysis of lignin in the secondary xylem cell wall in Populus. (a) Image setting. Intensity analyses for specific types of the cell wall can be performed in Fiji software. Open the selected picture and change the image to 8 bit. (b) Calculate the average photon counts for all measurements. Press “Analyze” and “Histogram” to calculate the average photon counts for all measurements. (c) (d) Obtained the ratio of the intensity value. Press the list, and the intensity values and counts will be shown. The total intensity values will be divided into 256 parts. From the 0 to 255 value, the intensity counts will be calculated for every tenth value. Then the ratio of the intensity value will be obtained by dividing the sum of ten counts by the total counts. (e) (f) Calculate the average intensity for selected cells. For each type of plant sample, at least three images were selected for intensity analysis. About 50 cells were selected for further analysis, press “Analyze” and “Measure” to calculate the average intensity for selected cells. Lignin (1600 cm−1) signals in each pixel are plotted, respectively, as intensity histograms and normalized by total intensity for better comparison.

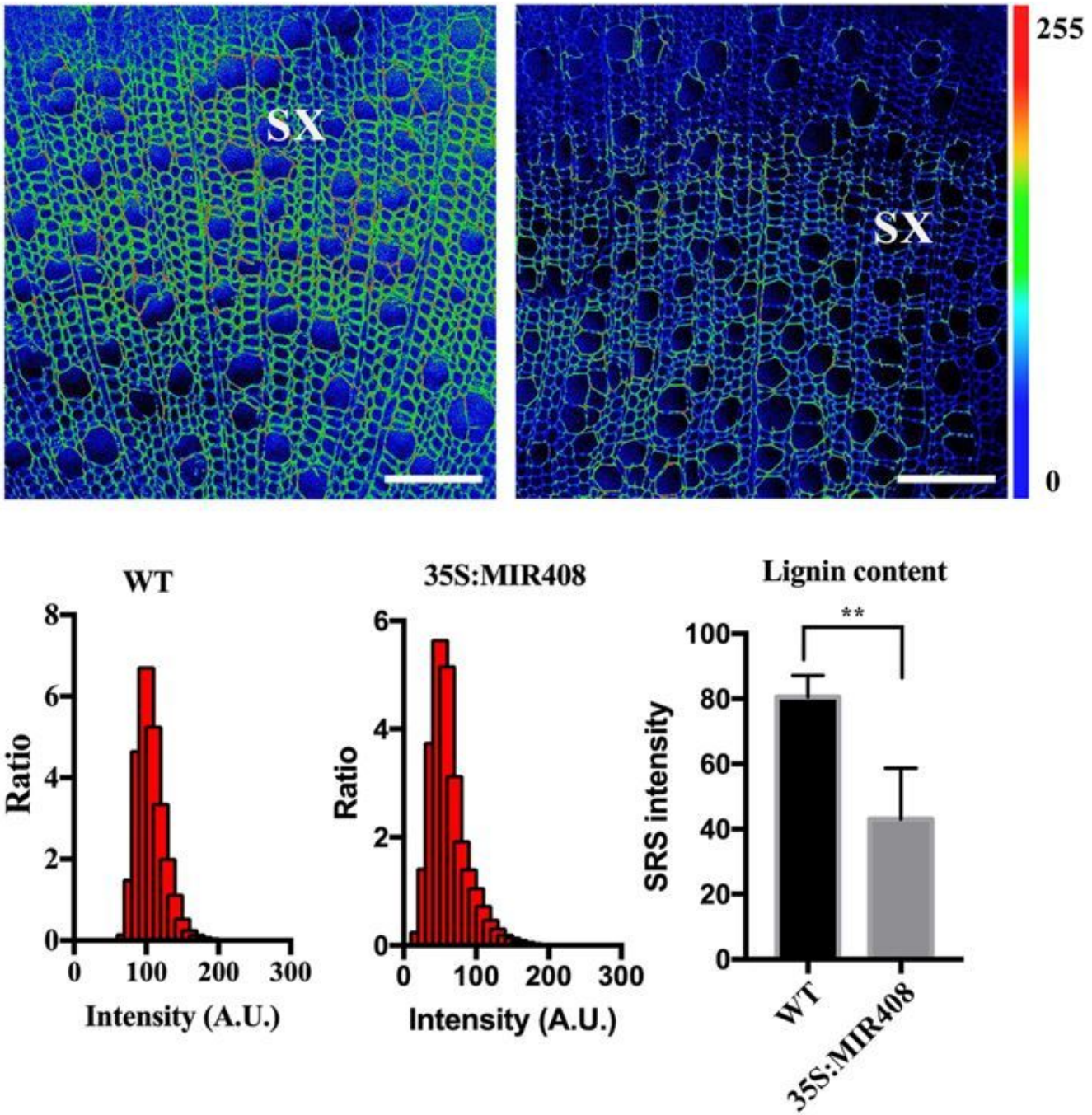

Figure 7

Example of image quantification of lignin in stems using SRS. Wild-type (WT) and 35S:MIR408 overexpressing Populus at 1600 cm-1, showing the lignin distribution. Color code indicates an increase of the signal intensity from blue to red. Scale bars are 50 μm.

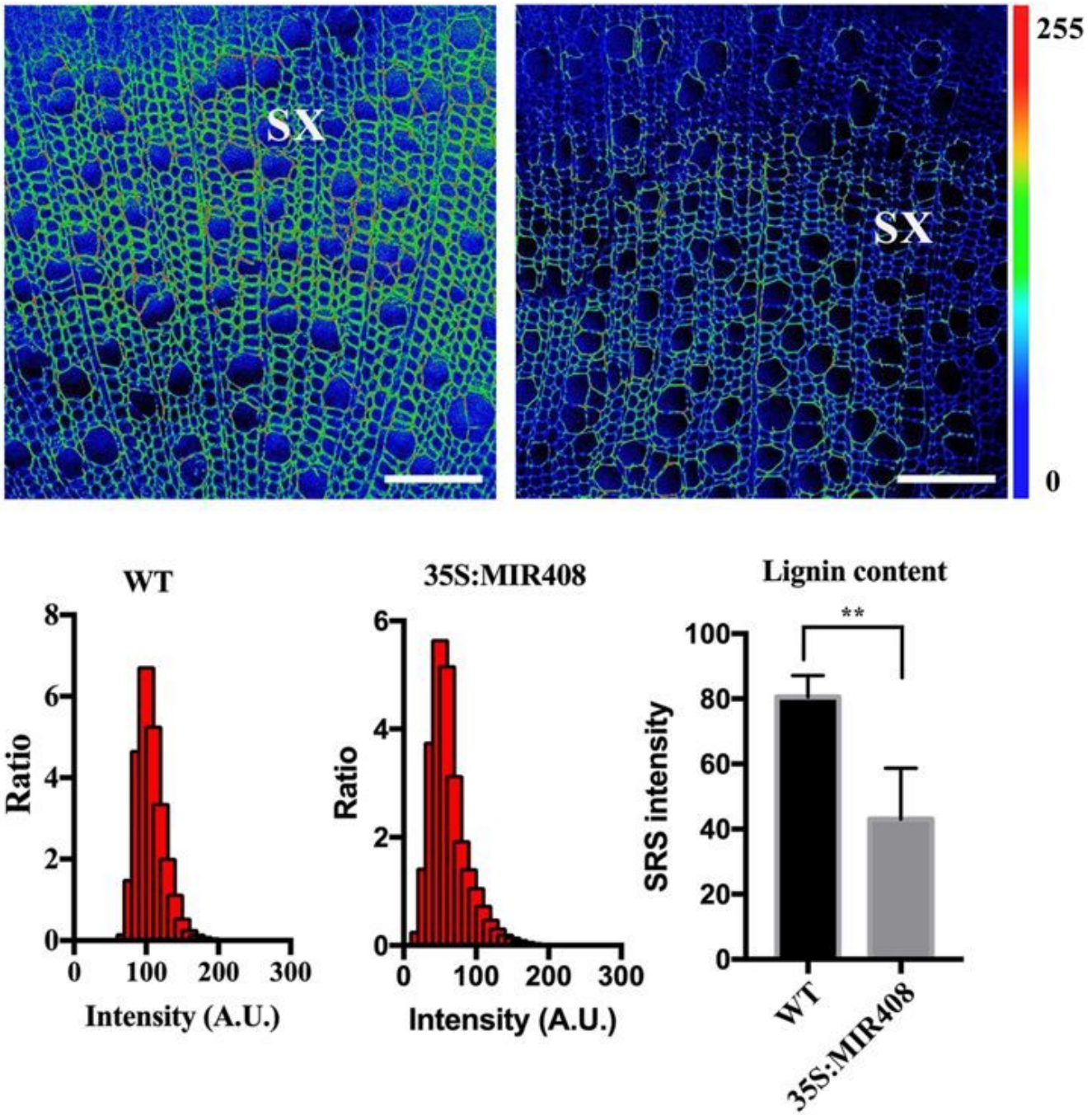

Figure 7

Example of image quantification of lignin in stems using SRS. Wild-type (WT) and 35S:MIR408 overexpressing Populus at 1600 cm-1, showing the lignin distribution. Color code indicates an increase of the signal intensity from blue to red. Scale bars are 50 μm.